Third AO4ELT Conference - Adaptive Optics for Extremely Large Telescopes
Florence, Italy. May 2013
ISBN: 978-88-908876-0-4
DOI: 10.12839/AO4ELT3.13167

THE LARGE BINOCULAR TELESCOPE AS AN EARLY ELT

J. M. Hill[1,2,a], P. M. Hinz[2], and D. S. Ashby[1]

[1]University of Arizona, LBT Observatory, 933 N Cherry Ave, Tucson AZ 85721, USA
[2]University of Arizona, Steward Observatory, 933 N Cherry Ave, Tucson AZ 85721, USA

Abstract. The Large Binocular Telescope (LBT) has two 8.4-m primary mirrors on a common AZ-EL mounting. The dual Gregorian optical configuration for LBT includes a pair of adaptive secondaries. The adaptive secondaries are working reliably for science observations as well as for the commissioning of new instruments. Many aspects of the LBT telescope design have been optimized for the combination of the two optical trains. The telescope structure is relatively compact and stiff with a lowest eigenfrequency near 8 Hz. A vibration measurement system of accelerometers (OVMS) has been installed to characterize the vibrations of the telescope. A first-generation of the binocular telescope control system has been deployed on-sky. Two instruments, LBTI and LINC-NIRVANA, have been built to take advantage of the 22.65-m diffraction baseline when the telescope is phased. This diffraction-limited imaging capability (beyond 20-m baseline) positions LBT as a forerunner of the new generation of extremely large telescopes (ELT). We discuss here some of the experiences of phasing the two sides of the telescope starting in 2010. We also report some lessons learned during on-sky commissioning of the LBTI instrument.

1. Introduction

The Large Binocular Telescope (LBT) [1] has two 8.4-m borosilicate honeycomb primary mirrors mounted side-by-side on a common AZ-EL mounting. These two mirrors provide the equivalent collecting area of an 11.8 m circular aperture. The telescope is located on Mt. Graham in southeastern Arizona, USA at an elevation of 3192 meters. The telescope is protected by a co-rotating rectangular enclosure as shown in Figure 1. The dual Gregorian optical configuration for LBT includes a pair of adaptive secondaries and a pair of tertiary flat mirrors. The adaptive secondaries [2] are working reliably for science observations as well as for the commissioning of new instruments. As discussed in Section 2, many aspects of the LBT telescope design have been optimized for the combination of the two optical trains to provide for the diffraction-limited resolution of a 22.65 meter telescope. In this sense, LBT takes a step beyond the 6-10 meter telescopes, and becomes an early ELT (extremely large telescope) with a diffraction baseline above 20 meters.

a e-mail : jhill@as.arizona.edu

Figure 1 - Photo of the nebulosity in the Mt. Graham winter sky above the dual apertures of the LBT enclosure taken by Babak Tafreshi (http://www.twanight.org) in November 2012. This is a 30-second integration on a DSLR modified to record H-alpha. The image used a tracking mount and a broadband skyglow filter. The rectangular LBT enclosure (29 x 28 x 25 m) corotates with the telescope in azimuth. Each of the 10 m wide shutter doors rolls to the side on rails.

2. Telescope Design Optimization

- The telescope has a compact Az-EL mechanical structure [3] with F/1.14 primary mirrors, and a direct load path from the primary mirrors to the C-Rings to the azimuth frame to the pier.
- High stiffness leads to higher eigenfrequencies (~8 Hz) of the structure. The LBT structure has served as a prototype for the structure of GMT (Giant Magellan Telescope) [4].
- Swing arms which support the secondary and tertiary mirrors and prime focus cameras allow rapid (10 min) reconfiguration of the telescope optics to follow changing sky conditions.
- Having two 8.4 meter primaries supported on the common mount avoids large distance pathlength compensation as a target tracks across the sky.
- LBT has a diffraction-limited baseline of 22.65 m (edge-edge) or 14.4 m (center-center). The two primary mirrors and the telescope elevation structure are shown in Figure 2.
- Aperture stops at the undersized adaptive secondaries reduce thermal background by providing cold sky around the edge of the secondaries. The instruments have internal cold stops near the image of the telescope pupil.

- Adaptive optics were designed in to the LBT telescope [5] from the start. By making the secondaries adaptive, we minimize the number of warm optical surfaces before the instruments.
- Gregorian optics allow testing the 672-actuator adaptive secondaries at finite conjugates. This makes testing simpler during optical fabrication, and during the daytime at the telescope.
- Smooth optics at small (cm) spatial scales match the best atmosphere. The optical surfaces are specified as structure functions with the tightest specifications at small spatial scales (1-10 cm). Larger spatial scale errors are readily removed by active and adaptive optics.
- Rapid thermal equilibration of the mirrors and surrounding structures minimizes local seeing.
- A facility system of 45 accelerometers mounted on the telescope structure and optics allows characterization of vibrations (OVMS) [6].
- Binocular telescope control system allows phased and un-phased observations with the two sides of the telescope. This control system has been in use for more than a year, although we are just now moving into more complex modes of observation such as mixed instruments observing the same target.

Figure 2 - A wide-angle view of the two 8.4 m primary mirrors of the LBT with the LBTI instrument mounted at the central focal stations. The red steel is the elevation structure of the telescope, and the green steel near the center is the support structure for the LBTI beam combiner and cameras.

3. Diffraction-Limited Instruments at LBT

A number of cameras have been used to record diffraction-limited images at LBT. A pair of IRTCs (Infrared Test Camera [7]) are useful for recording high-speed data during adaptive optics system commissioning. The PISCES [8] near-infrared imager has been used for some early science

observations with the FLAO (First Light Adaptive Optics [9]) system and its pyramid wavefront sensor. LBTI (Large Binocular Telescope Interferometer [10]) which combines the two sides of LBT includes the NOMIC camera for thermal nulling observations and LMIRcam [11] for near-infrared observations using the LBTI adaptive optics systems. LMIRcam has also provided some early science observations in parallel with LBTI commissioning. The PATHFINDER [12] experiment for the LINC-NIRVANA [13] wavefront sensor has been installed on the telescope in Spring 2013. The ARGOS [14] Rayleigh laser guide star system being installed in 2013 will add GLAO capability to the natural star FLAO adaptive optics system used in front of the two LUCI [15] near-infrared instruments. LINC-NIRVANA with binocular multi-conjugate adaptive optics is expected to arrive in 2015.

The following instruments have been used or will be used for diffraction-limited observations with adaptive optics at LBT:

- IRTC with FLAO (2010) – Commissioning adaptive optics with test camera
- PISCES with FLAO (2011-2012) – First one-eyed adaptive science observations
- LBTI with NOMIC (2010 -) – Commissioning Fizeau and Nulling modes at 8-12 microns
- LBTI with LMIRcam (2011 -) – Science observations at 2-5 microns
- L-N PATHFINDER (2013) – Commissioning multi-pyramid wavefront sensor
- LUCI with FLAO and ARGOS (expected 2014) – GLAO imaging and spectroscopy
- LINC-NIRVANA (expected 2015) – MCAO imaging at 1-2.5 microns

4. Phasing the Two Sides of LBT

4.1. Phasing Timeline

The following table represents the historical timeline of activities related to phasing the two sides of LBT:

- The first Fizeau fringed PSFs were obtained in October 2010 with LBTI and NOMIC.
- Fizeau fringed PSFs were obtained with LBTI and both NOMIC and LMIRcam in April 2012 with adaptive loops closed on both sides. An example at 4 microns is shown in Figure 3. Strehl ratios from the individual adaptive optics systems can be 70-90% on a bright star in H (1.6 microns), and higher at longer wavelengths.
- Engineering Nulling Fringes were obtained in February 2013 with LBTI and NOMIC (not yet with the phase loop holding the null stable).
- Science observations obtained with LBTI, LMIRcam and an APP (apodizing phase plate) coronagraph [16]; and also with NOMIC using non-redundant masking in February 2013.
- The phase stabilization loop will be closed for LBTI soon. It was delayed by a problem with the right adaptive secondary mirror in April 2013.

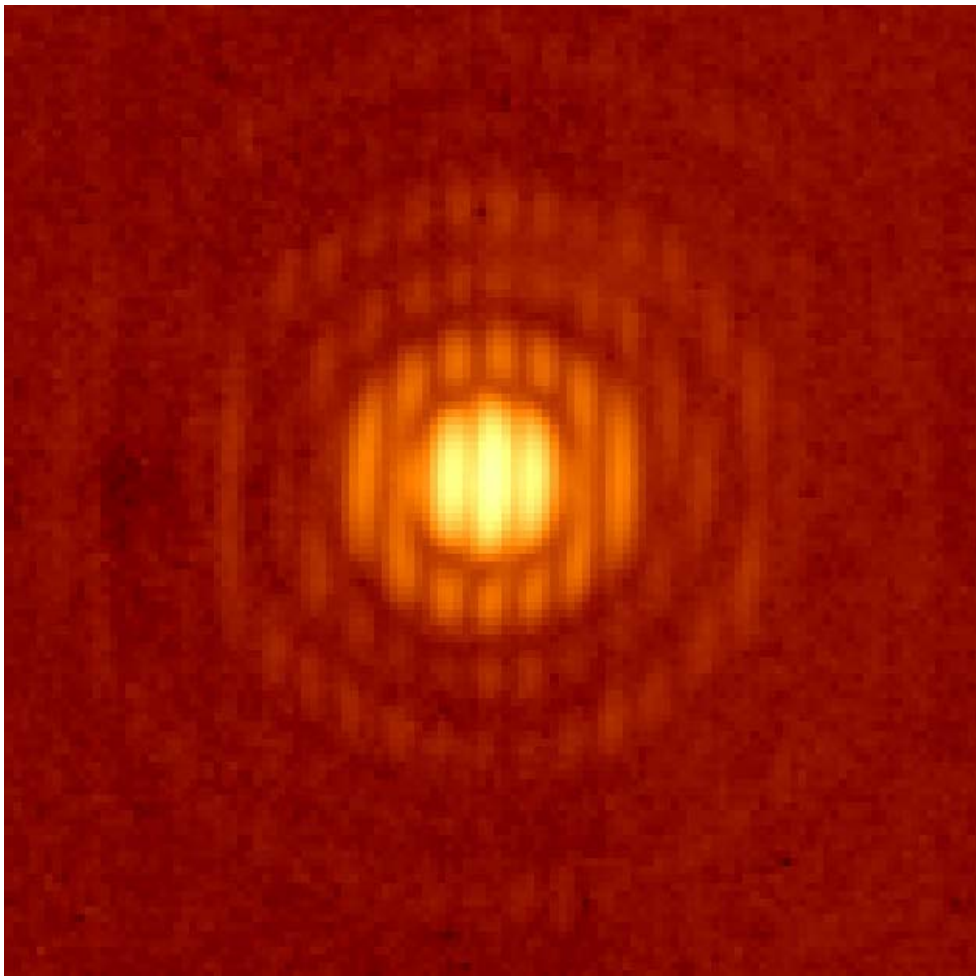

Figure 3 - LMIRcam image (courtesy A. Skemer) of the point spread function of the overlapped star images from the two sides of LBT. This is a stack of 50 selected short exposures (0.03 sec) of HD184786 at a wavelength of 4 microns (narrow band). The circular rings are the normal Airy diffraction pattern of a single 8.25 m diameter aperture (8.4 m primary w/ undersized secondary), and the vertical bars are the Young's fringes between the two apertures with 14.4 m center distance (corresponding to a resolution of 0.04 arcsec). The pixel scale is 11 mas/pixel.

4.2. Practical Lessons Learned

We have learned the following interesting and practical lessons on our way to phasing the two sides of LBT:

- Don't offload focus from the adaptive secondary shell as z-motion of the hexapod. This induces OPD errors in the conversion from shell bending focus to shell position focus. See the comparison in the plots of Figure 4.
- It is very efficient to use the fringes in the combined grism spectra from LMIRcam to adjust the pathlength between the two sides of the telescope to the white-light fringe. See the dispersed fringes in Figure. 5.
- The adaptive optics loops struggle to remain closed in seeing which is worse than 1.6 – 1.8 arcsec (depending on gain, number of modes, etc.). Poor seeing is a good opportunity to execute your non-adaptive backup program.

- The asymmetric structure of the LBT elevation and optics support structure makes for a challenging collimation model when the ambient temperature is rapidly changing. Temperature gradients in the telescope structure have proven difficult to incorporate into the optics collimation models.

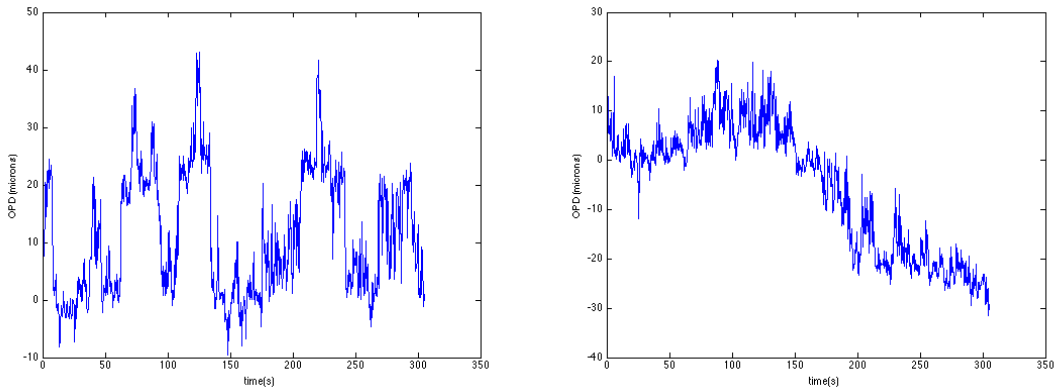

Figure 4 - These plots show the Optical Path Difference (OPD) between the two sides of LBT as measured by the dispersed fringes in LBTI/LMIRcam (see Figure 5). The first plot (left) has focus offloading turned on (accumulated focus on the adaptive shell is offloaded to hexapod piston) which creates noticeable jumps in OPD. The second plot (right) has focus offloading off (operated at very low gain) and the jumps in OPD have been suppressed into the atmospheric piston variations.

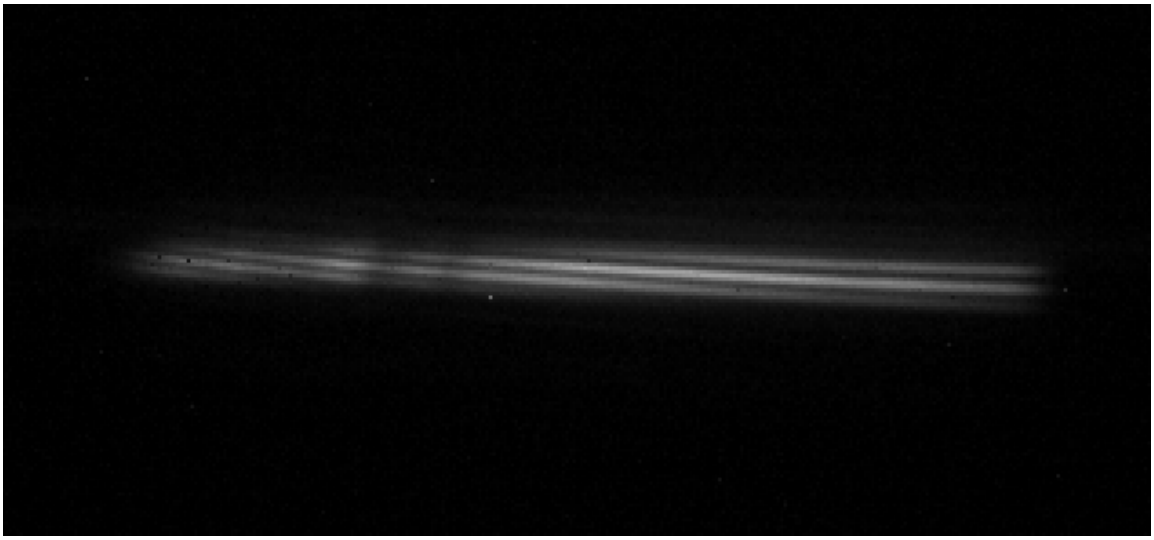

Figure 5 – Dispersed fringed PSF in the LBTI combined focal plane using the grism in LMIRcam. In this image, wavelength is dispersed left-right, and the spatial direction of the two primary mirrors is up-down.

5. Acknowledgements

We express our appreciation to Roger Angel, Nick Woolf, Peter Strittmatter and Piero Salinari for their technical vision and foresight to begin this project nearly 30 years ago.

The LBT is an international collaboration among institutions in the United States, Italy, and Germany. LBT Corporation partners are: The University of Arizona on behalf of the Arizona university system; Instituto Nazionale di Astrofisica, Italy; LBT Beteiligungsgesellschaft, Germany, representing the Max-Planck Society, the Astrophysical Institute Potsdam, and Heidelberg University; The Ohio State University, and The Research Corporation, on behalf of The University of Notre Dame, University of Minnesota, and University of Virginia.

Additional LBTO information may be found at http://www.lbto.org

6. References

1. J. M. Hill, et al., *Proc SPIE*, **8444**, pp. 1AH-12, (2012)
2. A. Riccardi, et al., *This conference*, (2013)
3. C. del Vecchio, L. Miglietta and W. B. Davison, *Proc SPIE*, **2199**, pp. 691-702, (1994)
4. P. McCarthy, *This conference*, (2013)
5. J. M. Hill and P. Salinari, *Proc SPIE*, **2199**, pp. 64-75, (1994)
6. M. Kürster, et al., *Proc SPIE*, **7734**, pp. 2Y-8, (2010)
7. I. Foppiani, et al., *Experimental Astronomy*, **31**, pp. 115-130, (2011)
8. D. W. McCarthy, et al., *PASP*, **113**, pp. 353-361, (2001)
9. S. Esposito, et al., *Applied Optics*, **49**, p. G174, (2010)
10. P. M. Hinz, et al., *This conference*, (2013)
11. J. M. Leisenring, et al., *Proc SPIE*, **8446**, pp. 4F-16, (2012)
12. A. R. Conrad, et al., *Proc SPIE*, **8447**, pp. 0V-10, (2012)
13. T. M. Herbst, et al., *Proc SPIE*, **8445**, pp. 0V-7, (2012)
14. W. Gässler, et al., *Proc SPIE*, **8447**, pp. 4I-11, (2012)
15. P. Buschkamp, et al., *Proc SPIE*, **8446**, pp. 5L-11, (2012)
16. M. A. Kenworthy, et al., *Proc SPIE*, **7734**, pp. 2P-11, (2010)